Modular tissue engineering for the vascularization of subcutaneously transplanted pancreatic islets

Alexander E. Vlahos[a], Nicholas Cober[a,b], and Michael V. Sefton[a,b,1]

[a]Institute of Biomaterials and Biomedical Engineering, University of Toronto, Toronto, ON M5S 3G9, Canada; and [b]Department of Chemical Engineering and Applied Chemistry, University of Toronto, Toronto, ON M5S 3G9, Canada

Edited by Kristi S. Anseth, Howard Hughes Medical Institute, University of Colorado Boulder, Boulder, CO, and approved July 21, 2017 (received for review November 21, 2016)

The transplantation of pancreatic islets, following the Edmonton Protocol, is a promising treatment for type I diabetics. However, the need for multiple donors to achieve insulin independence reflects the large loss of islets that occurs when islets are infused into the portal vein. Finding a less hostile transplantation site that is both minimally invasive and able to support a large transplant volume is necessary to advance this approach. Although the s.c. site satisfies both these criteria, the site is poorly vascularized, precluding its utility. To address this problem, we demonstrate that modular tissue engineering results in an s.c. vascularized bed that enables the transplantation of pancreatic islets. In streptozotocin-induced diabetic SCID/beige mice, the injection of 750 rat islet equivalents embedded in endothelialized collagen modules was sufficient to restore and maintain normoglycemia for 21 days; the same number of free islets was unable to affect glucose levels. Furthermore, using CLARITY, we showed that embedded islets became revascularized and integrated with the host's vasculature, a feature not seen in other s.c. studies. Collagen-embedded islets drove a small (albeit not significant) shift toward a proangiogenic CD206^{+}MHCII^{-}(M2-like) macrophage response, which was a feature of module-associated vascularization. While these results open the potential for using s.c. islet delivery as a treatment option for type I diabetes, the more immediate benefit may be for the exploration of revascularized islet biology.

pancreatic islets | subcutaneous transplant | tissue engineering | islet revascularization | CLARITY

Pancreatic islet transplantation is a promising treatment for those living with type 1 diabetes (1, 2), but this therapy has limitations (3, 4). Using current methods (portal vein infusion), up to 60% of transplanted islets are lost within the first 3 d (5), and thus islets from multiple donors are required to achieve normoglycemia (6). Islet engraftment is adversely affected by the blood-mediated inflammatory response (7) and a lack of vascularity, subjecting the islets to ischemia.

The s.c. site has been considered as an alternative site for islet transplantation because of its large (albeit not necessarily readily accessible) size, and s.c. injection could limit procedural risk compared with other sites. However, because s.c. vascularity is poor (8), various strategies to vascularize the site are being explored (9, 10), e.g., the use of mesenchymal stromal cells (MSC) (11). With the perspective that the underlying problem is hypoxia, Ludwig et al. (12) created an implantable chamber equipped with a refillable oxygen chamber to support s.c. islet transplantation. Alternatively, others have used a two-step protocol (13, 14) in which a cavity is prepared in the s.c. space; islets are then added after several weeks' delay to minimize the impact of the inflammatory response while perhaps generating a prevascularized site.

Pancreatic islets are highly susceptible to apoptosis due to insufficient oxygen and nutrient diffusion (15). After transplantation it is critical that the pancreatic islets become rapidly revascularized and integrated with the host's systemic vasculature to achieve glucose homeostasis (16). While revascularization has been observed in vascularized extrahepatic sites such as the small-bowel mesentery (10) and kidney capsule (17), revascularization and anastomosis with the host's vasculature have not previously been shown in the s.c. space. Such integration is presumed to be necessary for long-term graft survival.

Modular tissue engineering is a bottom-up approach to create vascularized tissue implants that can be injected s.c. (18). Submillimeter collagen cylinders ("modules") are coated with endothelial cells (EC) (18); the EC migrate and vascularize the s.c. site as the modules remodel. With MSC embedded in modules as support cells, a mature s.c. vascular bed is created within 14–21 d of transplantation in both immune-suppressed Sprague–Dawley rats (19) and immune-compromised SCID/beige (bg) mice (20).

The objective of this study was to show that pancreatic islets embedded in endothelialized modules and injected s.c. became revascularized and returned streptozotocin-induced diabetic SCID/bg mice to normoglycemic levels. The protocol is illustrated in Fig. S1. The effect of adding adipose-derived mesenchymal stromal cells (adMSC) or omitting human umbilical vein endothelial cells (HUVEC) was also tested. We used the CLARITY protocol (21, 22) to image the entire explant and show the anastomosis of the pancreatic islets with the host's systemic vasculature. In addition, we used flow cytometry to characterize the inflammatory response, which is a key driver of vascularization but may also limit islet survival after transplantation.

Results

Restoration of Normoglycemia. Pancreatic islets harvested from Wistar rats (750 islet equivalents, IEQ) embedded in HUVEC-coated modules were sufficient to restore normoglycemia (glucose <11.1 mM) in five of six streptozotocin-induced diabetic SCID/bg mice (islet modules with HUVEC, green lines in Fig. 1 *A* and *B*). In four of these implants, normoglycemia was obtained within 10 d after implantation (Fig. 1*B*). As expected, free islets (not embedded in modules) were unable to restore normoglycemia. Islets embedded in collagen but without EC

Significance

In this study we show that pancreatic islets embedded in modules coated with endothelial cells and injected under the skin return streptozotocin-induced diabetic SCID/beige mice to normoglycemia. The transplanted islets became revascularized and directly integrated with host's vasculature, a feature not seen previously in the subcutaneous space. These implants were also retrievable, an important clinical consideration. The success here means that islet transplantation can move away from inhospitable sites such as the peritoneal cavity or the liver.

Author contributions: A.E.V., N.C., and M.V.S. designed research; A.E.V. and N.C. performed research; A.E.V. and N.C. analyzed data; and A.E.V., N.C., and M.V.S. wrote the paper.

The authors declare no conflict of interest.

This article is a PNAS Direct Submission.

[1]To whom correspondence should be addressed. Email: michael.sefton@utoronto.ca.

This article contains supporting information online at www.pnas.org/lookup/suppl/doi:10.1073/pnas.1619216114/-/DCSupplemental.

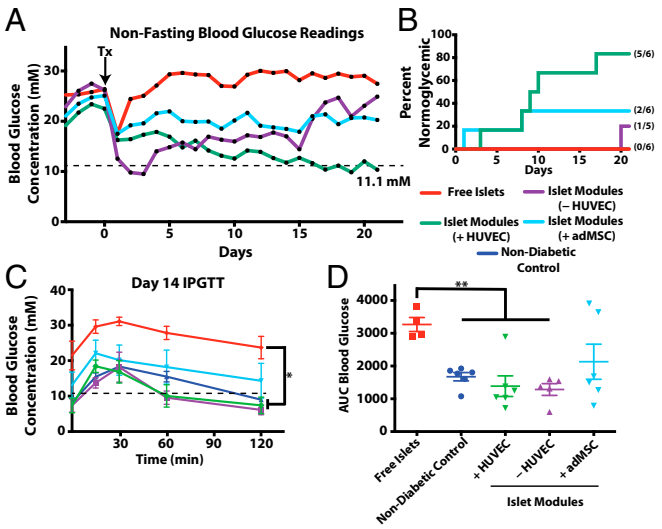

Fig. 1. The s.c. modular islet transplants with HUVEC restored normoglycemia. (*A*) Shown are average nonfasting blood glucose levels for diabetic mice implanted with free islets ($n = 6$) or islets in modules with (+HUVEC) ($n = 6$) or without (–HUVEC; collagen only; $n = 5$) HUVEC or with adMSC and HUVEC (+adMSC) ($n = 6$). While all free-islet recipients remained hyperglycemic for the entire experiment, islet modules with HUVEC were able to lower glucose levels to normal in all but one animal. Individual glucose values are shown in Fig. S2. Islet modules without HUVEC or with adMSC and HUVEC had some therapeutic effect on the average glucose levels; however, most of these animals remained hyperglycemic. The dotted line represents the threshold for normoglycemia (11.1 mM). (*B*) Kaplan–Meier plot showing when animals became normoglycemic. Not shown are animals that became normoglycemic but reverted to hyperglycemia within the 21-d observation period. Mice implanted with islet modules with HUVEC reversed diabetes significantly faster than the free-islet group ($P = 0.0043$, log-rank, Mantel-cox test) or the group with islet modules without HUVEC ($P = 0.0196$, log-rank, Mantel–Cox test). Numbers in parentheses indicate the fraction of animals that are shown in this plot. (*C*) IPGTT glucose profile at day 14. Animals were fasted for 4 h before IPGTT was performed. A repeated-measures ANOVA with a Games–Howell post hoc test revealed a significant difference between the profiles of the free-islet group and the nondiabetic control and the groups with islets embedded in modules with or without HUVEC. (*D*) AUC analysis confirmed that mice in the free-islet group were intolerant of the glucose challenge and that there was a significant difference between the free-islet group and both groups receiving islets embedded in modules with ($n = 6$) or without ($n = 5$) HUVEC. There was no significant difference among the islet module groups. $^*P < 0.05$, $^{**}P < 0.01$.

were able to return one mouse (of five) to normoglycemic levels at day 20, but the majority of the animals remained hyperglycemic (islet modules without HUVEC, purple line in Fig. 1*A*; also see Fig. S2]. Animals that were transplanted with islets and adMSC embedded in endothelialized modules (islet modules with adMSC) received some beneficial effect of reduced blood glucose levels in the diabetic animals (two of six animals returned to normoglycemia by day 8), but this treatment was not as effective as islet modules with HUVEC but without adMSC. Implants in mice that had returned to normoglycemic levels were removed without the mice being killed, and these animals reverted to diabetic pretransplantation levels (Fig. S3). Viable islets from the modules explanted at day 21 stained positively for insulin (Fig. S4*A*), and the islet module implants, with or without HUVEC, had the greatest density of insulin-positive pixels within the implant area (Fig. S4*B*).

Islets embedded in collagen modules (with or without HUVEC) had i.p. glucose-tolerance test (IPGTT) response profiles comparable to nondiabetic controls (Fig. 1*C*) as well as similar area under the curve (AUC) (Fig. 1*D*) at day 14. In comparison, diabetic mice implanted with free rat islets (no modules) were intolerant of the glucose bolus (high AUC, red line in Fig. 1*C*). Islets embedded in modules with adMSC were able to respond partially to the glucose bolus, although some of these mice had not returned to normoglycemia at 120 min postinjection.

Effects on Vascularization. The $CD31^+$ vessel density in explants was similar among the different module groups at day 21 (Fig. 2), even in those with islets but without adMSC; free-islet explants could not be reliably found and analyzed. As expected, smooth muscle actin-positive (SMA^+) vasculature was present throughout all the modular implants at day 21, suggesting that the vessels were mature (Fig. 2*A*, *Lower Row* and Fig. S5). The module-associated vasculature was mainly host-derived at day 21, since there was a lack of *Ulex europeus* agglutinin-1–positive ($UEA\text{-}1^+$) vessels in the histological analysis (Fig. S6*A*).

While there were no observable differences in the total amount of vessels among the different module groups at day 21 (Fig. 2*B*), islet modules with HUVEC at day 7 and 14 had significantly more $CD31^+$ vessels than islet modules without HUVEC ($P < 0.05$) (Fig. 2*B*). In addition, there was a distinct shift in the chimeric nature of module-associated vasculature at day 7, when 20% of vessels were $UEA\text{-}1^+$, to an entirely host-derived module-associated vasculature at day 14 with few $UEA\text{-}1^+$ vessels (Fig. S6*B*).

Intraislet Vasculature. In addition to counting vessels around individual modules, we also observed $CD31^+$ cells within embedded islets at day 21 (Fig. 3*A*, *Middle*), suggesting that islets retained their vasculature or became revascularized. Although the number of insulin-positive viable islets among the groups was different (Fig. S4*B*), comparisons among the different modular groups revealed no significant differences in the percentage of $CD31^+$ pixels within the interior of the islets that were present at day 21 (Fig. S7), suggesting that the islets that were found by histology had similar $CD31^+$ content.

To confirm that these intraislet vessels had anastomosed with the module-associated vasculature and were perfusable at day

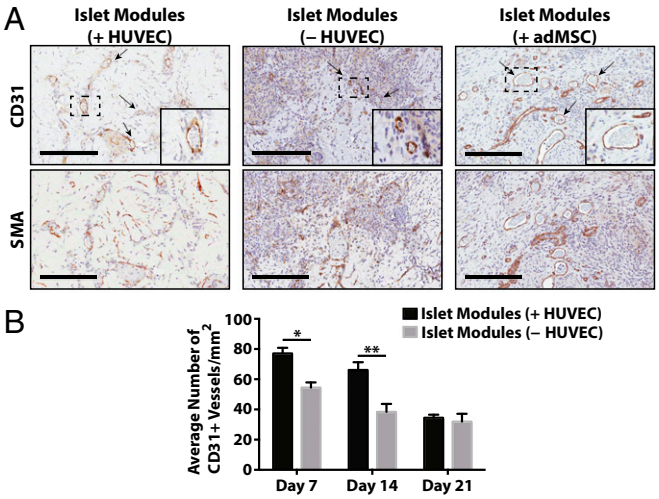

Fig. 2. Module-associated vascularization. (*A*) Module-associated vasculature was characterized by staining with CD31 and SMA in serial sections at day 21. $CD31^+$ vessels (black arrows, *Upper Row*) were present in all groups, including the without-HUVEC group, and many of these vessels were also positive for SMA, suggesting that the vessels were mature. (Scale bars: 200 μm.) (*B*) CD31 vessel counts. There were significantly more vessels when islet modules were coated with HUVEC ($n = 6$) than without HUVEC ($n = 5$) at days 7 and 14 (two-sided *t* test). At day 21 the density of $CD31^+$ vessels was similar between the two module groups ($P > 0.05$). Islet modules without HUVEC degraded over time, and not many implants could be found at day 21. $n = 5$ for islet modules with HUVEC and $n = 2$ for islet modules without HUVEC at day 21. $^*P < 0.05$, $^{**}P < 0.01$; error bars indicate SEM.

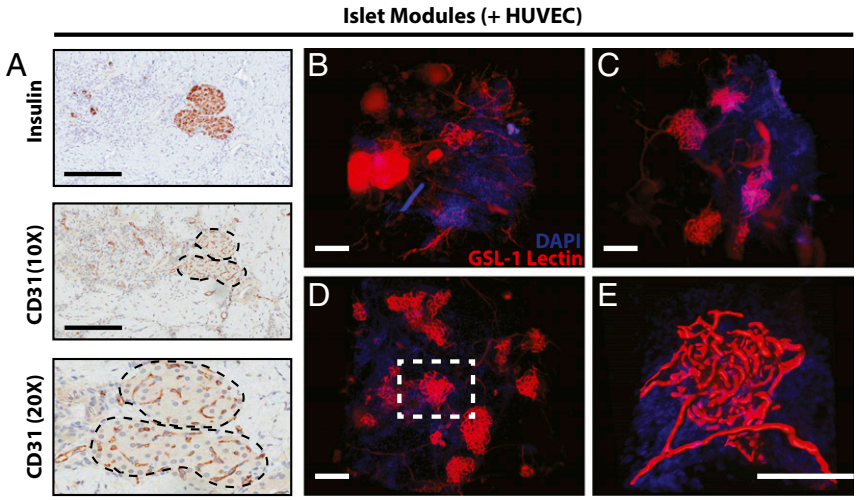

Fig. 3. Islets in endothelialized modules were revascularized. (*A*) Islets embedded within endothelialized modules had CD31$^+$ staining within the interior of the islets at day 21. (Scale bars: 200 μm.) (*B–D*) CLARITY-processed islet modules with HUVEC at day 7 (*B*), day 14 (*C*), and day 21 (*D*) show islet revascularization over time. (*E*) An embedded rat islet (white dashed box in *D*) was computationally mapped using IMARIS to visualize revascularization of the islet and its vasculature morphology. Movies are shown in *Supporting Information*. (Scale bars: 150 μm.)

21, *Griffonia simplicifolia* lectin 1 (GSL-1) conjugated to Alexa-555 was injected via the tail vein of the animal. Whole-islet module (+HUVEC) implants at days 7, 14, and 21 were processed using CLARITY (21, 22) and imaged using light-sheet microscopy. Islets were identified by their extensive vascular morphology compared with the module-associated vasculature (Fig. 3). At day 7, the module-associated vasculature network had begun to integrate with the embedded islets (Fig. 3*B*), but the islet vasculature was not entirely perfusable at this time point. The GSL-1 lectin was seen to "pool," being unable to be removed during the PBS perfusion step (Fig. 3*B* and Movie S1). At days 14 and 21, these GSL-1 pools were not seen, and intraislet vessels became perfusable (Fig. 3 *C* and *D* and Movies S2 and S3).

Embedded islets became fully vascularized by day 21, and the vessels were computationally mapped using IMARIS to visualize the direct integration of the modules with the host vasculature (Fig. 3*E*): intraislet vessels occupied 20 ± 3% (average of eight islets) of the total islet volume (Fig. S8*C*).

Inflammatory Response. Whole implants were analyzed by flow cytometry to assess the recruitment of neutrophils and macrophages to implants at day 7 and 14. The focus was on the effect of islets in islet modules with or without HUVEC, but with no adMSC compared with a no-islet control (HUVEC-coated modules without islets); these groups with islets were best at regulating blood glucose.

Macrophage polarization toward a proinflammatory phenotype (M1) or an anti-inflammatory repair phenotype (M2) was assessed by the expression of known M1 and M2 markers (MHCII and CD206, respectively). At day 7, a small, albeit not significant, shift was observed toward CD206$^+$MHCII$^-$ (M2-like) macrophage in islet modules, with and without HUVEC, compared with no-islet controls (Fig. 4*C*). This progression continued to day 14, while the no-islet controls were shifting toward a CD206$^+$MHCII$^+$ double-positive phenotype (Fig. 4*E*). At day 7 more neutrophils (CD11b$^+$Ly6G$^+$) (Fig. 4*A* and Fig. S9*A*) were observed with islet modules than with the no-islet control (Fig. S9*A*), as was a larger (albeit not significant) proportion of CD11b$^+$F4/80^{low} monocytes. The large population of neutrophils (and perhaps monocytes) observed at day 7 suggested that inflammation was sustained much longer than normally seen with modules without islets; without islets, these cells were previously seen to resolve by day 3. On the other hand, the presence of these cells may indicate the presence of leaky blood vessels and blood pools at this time (Fig. 3*B*). At day 14, neutrophil numbers decreased to expected levels, and few F4/80^{low} cells were observed (Fig. 4*B* and Fig. S9*B*), consistent with the absence of blood or GSL-1 pools.

Discussion

Modular Tissue Engineering and Islet Transplantation. The streptozotocin-induced diabetic SCID/bg model enabled us to test the hypothesis that module-associated vascularization enables s.c. islet delivery and the return to normoglycemia. Unlike free islets, islets embedded within modules with HUVEC had a beneficial effect on glucose levels when transplanted into the s.c. space of streptozotocin-induced diabetic SCID/bg mice (green line in Fig. 1*A*); the majority of the animals became normoglycemic within ∼10 d, which was sustained for the entire observation period. By day 14, islets were able to respond to a glucose challenge in a manner comparable to nondiabetic mice (Fig. 1 *C* and *D*). Islets were structurally intact and demonstrated insulin-positive staining at day 21 (Fig. S4*A*), suggesting that modules provided a suitable environment for the survival and function of the transplanted islets. In addition, the vessels at day 21 in the islet-treatment groups were mature (i.e., invested with SMA$^+$ cells) (Fig. 2*A*) and entirely host-derived (Fig. S6).

The s.c.-injected islet modules with HUVEC self-assembled to form a tissue "organoid." This construct remained intact and retrievable (Fig. S3) due to the presence of the HUVEC, which protected the constructs from collagen degradation. This retrievability in the event of complications is an important clinical consideration for future work using alternative insulin-producing cells such as stem cell-derived pancreatic progenitor cells.

Simply embedding islets within collagen modules (without other cells) offered some impact on glycemia, but these mice reverted to hyperglycemia within the 21-d observation period (purple line in Fig. 1*A* and see Fig. S2). Islet modules without HUVEC degraded over time (histology was feasible on only two of five implants due to the loss of module integrity), and the islets may have lost structure (and function) due to collagen degradation (23, 24), causing the eventual return to hyperglycemic levels. The IPGTT results were similar at day 14 regardless of treatment group (Fig. 1*C*), suggesting that there was still sufficient islet mass in the no-HUVEC group at day 14, consistent with the nonfasting near-normal glucose levels (Fig. S2) and reports that collagen is beneficial for maintaining intact islet structures (23, 25). However, islets in the collagen-alone group failed after day 14, rendering this group a less favorable

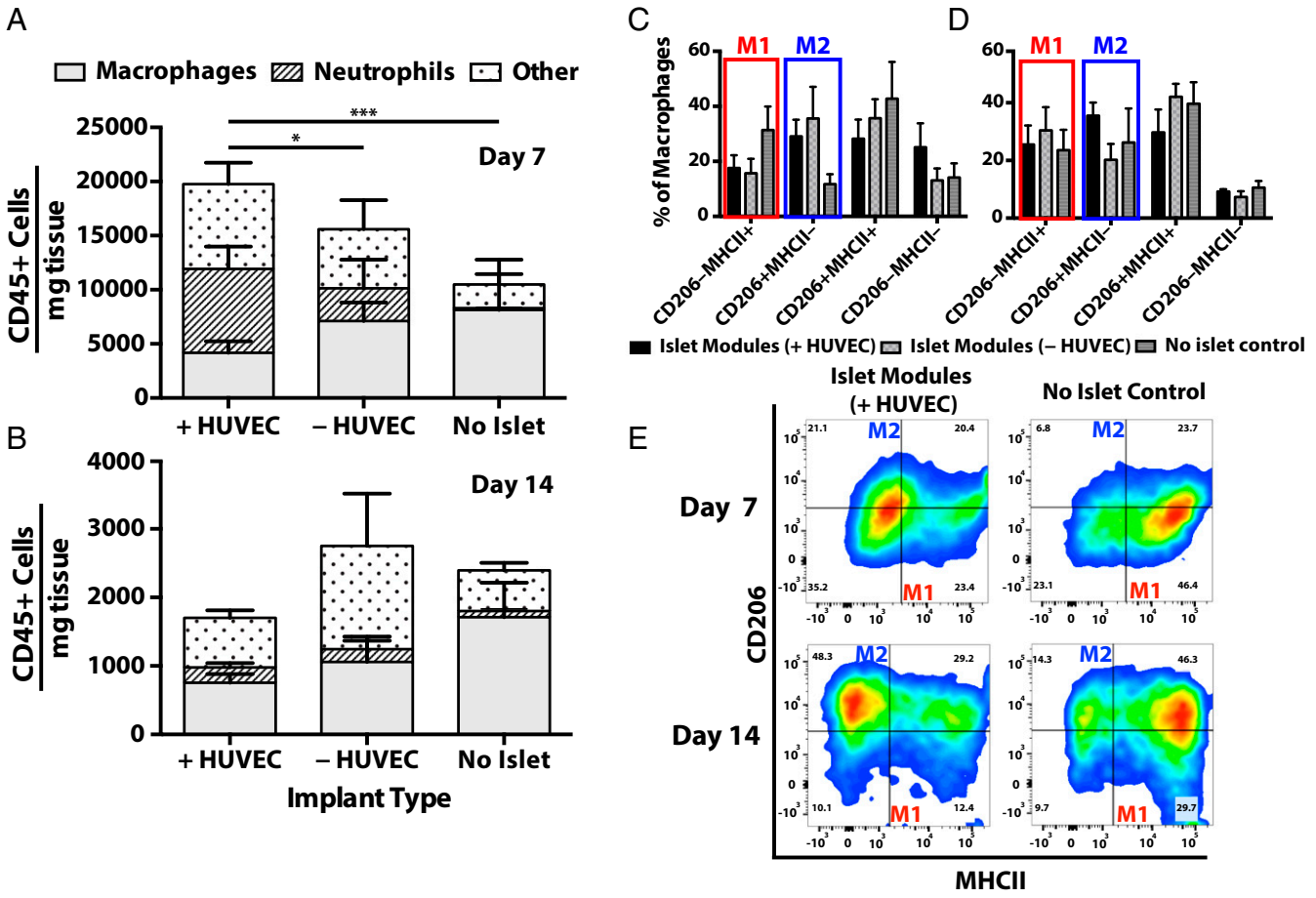

Fig. 4. Inflammatory response associated with transplanted islets. (*A* and *B*) Many CD45$^+$ cells were seen at day 7 with islet-containing modules; this response decreased by day 14. Shown is the distribution of CD45$^+$ cells found within explants for islet modules with and without HUVEC and the no-islet (+HUVEC) control at day 7 (*A*) and day 14 (*B*). There were significantly more neutrophils present in islet modules with HUVEC than in islet modules without HUVEC (*$P <$ 0.05) and in the no-islet control modules (***$P < 0.0005$) at day 7. (*C*–*E*) Macrophage polarization was assessed by coexpression of CD206 and MHCII, where M1-like macrophages are CD206$^-$MHCII$^+$ and M2-like macrophages are CD206$^+$MHCII$^-$. Quantification of macrophage phenotype at day 7 (*C*) and day 14 (*D*) with representative flow plots of islet modules with HUVEC and no-islet controls at day 7 and day 14 (*E*). Error bars represent mean ± SEM, $n = 5$ for all groups, except in the day 7 no-islet control ($n = 3$) and in the day 14 islet module with HUVEC and no-islet control ($n = 4$).

option than islet modules with HUVEC, although better than free islets alone.

The addition of adMSC did not have a beneficial effect on the ability of the transplanted islets to return diabetic mice to normoglycemia (Fig. 1*B*). Some literature supports the use of MSC in islet transplantation protocols (26, 27), although this may depend on MSC source (28) and dosage. There was also no substantive need for adMSC as a vascular support cell here (in the presence of islets), unlike previous module studies where they were critical for promoting early HUVEC survival (20). adMSC may not offer any vascularization advantage in the presence of the islets, given that islets also release proangiogenic growth factors (e.g., VEGF-A) in response to hypoxia (29). Perhaps the adMSC were competing with the embedded islets for nutrients and oxygen at critical early time points.

s.c. Islet Delivery. The s.c. space is being pursued as an alternative site for the transplantation of pancreatic islets (13, 26) because it can support a large, retrievable transplant volume. The primary challenge of the s.c. site for the transplantation of pancreatic islets is ensuring proper vascularization. Other groups have attempted to use the s.c. site with different systems, but these typically need excess islets to achieve glycemic control due to poor vascularization and a corresponding lack of direct integration with the host (28, 30, 31). For example, Hirabaru et al. (30) used an MSC sheet to s.c. transplant 2,000 rat islets to rectify diabetes in SCID/bg mice for 28 d, but they were unable to achieve a therapeutic effect with a lower dosage of islets. Similar islet numbers (2,000–3,000) are reported by others for s.c. normoglycemia in xenograft models in immune-compromised mice (13, 30, 32). The success (or lack of success) of xenogeneic islet transplantation, largely in the kidney capsule, has been reviewed elsewhere (33). With modules containing HUVEC, 750 IEQ was sufficient to restore normoglycemia in this immune-compromised xenograft model.

To improve vascularization (and reduce islet needs), some groups have attempted to prevascularize the s.c. site in a first step for subsequent islet transplantation in a second step (13, 14, 26, 34). These strategies were effective at prolonged glycemic control [some >100 d (13)] with low numbers of syngeneic islets, but it is unclear if they achieved the intended prevascularization in all cases. For example, based on published micrographs, the vessel density appears much less than that we typically see with modular tissue engineering (20). In addition, these groups often required 20–50 d after islet delivery (13, 14, 35) to see a return to normoglycemia (compared with ∼10 d for islet modules with HUVEC), perhaps highlighting the limited vascularization of their prevascularized sites.

We have yet to use autoimmune diabetes models such as the NOD mouse or the NRG Akita mouse (36), nor have we explored transplants over longer times (e.g., 3 mo). More importantly, these mice do not have the impaired vascularity that is associated with human diabetes. It has been reported that 8–16 wk of hyperglycemia is required to observe features of diabetic neuropathy in rodents (37), which may be indicative of when vascular pathology also occurs. Our approach provides a platform that can be used to understand the relationship between s.c. islet graft viability and revascularization in this and, we expect, other animal models of greater translational significance.

Islet Revascularization and Integration. Integration of the transplanted rat islets with the host's vasculature is important for glucose-sensing and insulin-secretion activity of the beta cells (38). Islet modules with HUVEC provided the most consistent and robust return to normoglycemia in our study, which we attribute to islet revascularization and integration. At day 21, $CD31^+$ staining was present within structurally intact islets of our s.c. implants (Fig. 3*A*), consistent with the presence of an intraislet vasculature. To directly show that these intraislet vessels had anastomosed with the host's vasculature, we adapted a CLARITY protocol (39) with animals that had been injected with GSL-1 lectin via the tail vein (Fig. 3 *B*–*E* and Movies S1–S3). Islets were identifiable by their distinct vasculature morphology (clusters of small GSL-1^+ vessels), which were integrated with the host vasculature (Fig. 3 *D* and *E*). Such an integrated and perfusable vasculature was a highlight here but was not hitherto a feature of previous s.c. implant studies (13, 30).

CLARITY processing also showed that vessel remodeling was complete between days 7 and 14. The vasculature was perfusable (Fig. 3*C* and Movie S2) and invested with SMA^+ cells (Fig. S10, *Lower Row*) by day 14 with the pools of GSL-1 attributed to leaky, immature vessels that were seen at day 7 (Fig. 3*B* and Movie S1) no longer visible. The time to achieve revascularization of the pancreatic islets (between days 7–14) is consistent with the time to return to normoglycemia (~10 d). The volume of intraislet vasculature relative to total islet volume (~20%) (Fig. S8) was comparable to that of freshly isolated rodent islets [17% of total islet volume (40)]. This maintenance and integration of the intraislet vasculature has been proposed to be critical for long-term graft survival (15) and has not been shown previously with s.c. islet transplants.

Innate Immune Response. There were differences in $CD45^+$ cell numbers at day 7 in islet modules with HUVEC relative to no-islet controls (Fig. 4*A*), but this difference subsided by day 14 (Fig. 4*B*). The presence of islets elicited more inflammatory cells relative to the standard module implant (41). This early increase in cell number is consistent with reports that islets will recruit leukocytes triggered by a response similar to the instant blood-mediated inflammatory response (42). There is evidence that VEGF-A (29) and IL-8 (43) secreted by islets are potent drivers not only of angiogenesis but also of the recruitment of $CD45^+$ leukocytes in the form of neutrophils (29) and monocytes/macrophages (44). Surprisingly a large population of neutrophils was still present at day 7 in implants containing embedded islets (Fig. 4*A* and Fig. S9*A*), even though neutrophils typically decline after the first 48 h of inflammation (45).

A fundamental dilemma in promoting vascularization of islet transplants is that the inflammation that underlies vascularization, as noted above, can impair islet function. Mitigating this concern, we note that islets embedded in modules (with or without HUVEC) had a higher fraction of M2-like macrophages ($CD206^+MHCII^-$) at day 7 compared with the no-islet control (Fig. 4 *C* and *E*, *Upper*), although the differences were not significant. At day 14, macrophages predominately expressed the M2-like phenotype (Fig. 4 *D* and *E*, *Lower*) in all groups. Previous studies have shown a positive effect of M2-like macrophages on beta cell survival (46) and proliferation (47). Perhaps this stronger bias toward M2 macrophages was a factor in islet survival and vessel integration. The s.c. modules may allow the study of immune-modulatory strategies, e.g., small molecule inhibitors (48) or cells (49), to promote graft survival or tolerance in immune-competent animal models.

Conclusion

The s.c. injection of rat pancreatic islets embedded in endothelialized modules was able to return streptozotocin-induced diabetic SCID/bg mice to normoglycemia. HUVEC seeded on the modules was important for vascularization at early time points and for preserving the structural integrity of the modular implants. Islets embedded in endothelialized modules became revascularized, and whole-explant imaging showed that the intraislet vasculature had integrated with the host's vasculature by day 14, a feature not shown in previous s.c. studies. In addition, embedded islets experienced an inflammatory response that consisted of mainly M2-like macrophages, which was considered important for tissue remodeling and vascularization, although the high neutrophil response at day 7 suggests that there may be a need to modulate other aspects of early inflammation to protect islet viability. Module-based vascularization in which the transplanted islets become integrated with the host vasculature has enabled the s.c. site to be a suitable option for islet transplantation.

Materials and Methods

Islet Isolation. Primary rat islets were harvested from 12-wk-old Wistar rats using a previously described protocol (50). IEQ were then calculated based on volumetric assumptions (51). Primary rat islets were cultured in RPMI-1640 medium (Gibco) supplemented with 10% FBS (Gibco) and 1% penicillin-streptomycin (Pen/Strep) (Gibco). For the in vivo studies, eight independent islet isolations and transplantations were performed. Each isolation generated enough islets (2,800) for three implants, spanning multiple test groups.

Module Fabrication. Modules were fabricated as before (20). HUVEC-coated islet modules were produced by embedding rat islets (750 IEQ) without adMSC. In addition, HUVEC-coated modules that contained adMSC (10^6 cells/mL collagen solution; Lonza) or no embedded cells were produced. For a complete list of the different cell compositions used for the modules in this study, please refer to Table S1.

Module Transplantation. All animal experiments and surgeries were performed at the University of Toronto and were approved by the Faculty of Medicine Animal Care Committee. SCID/bg mice (5–6 wk old; Charles River) were made diabetic through a single i.p. injection of streptozotocin (200 mg/kg) (Sigma-Aldrich) 1 wk before transplantation. Blood glucose was measured via the tail vein with a glucose meter (OneTouch UltraSmart; LifeScan), and animals were considered diabetic when their blood glucose levels exceeded 20 mM for two consecutive daily readings.

The modules were rinsed with PBS (Gibco) and s.c. injected into the dorsum using an 18-G needle, as previously described (19, 20). Animals were housed individually in sterile conditions and were provided with irradiated food and water. Nonfasting blood glucose levels were monitored daily until the implants were harvested at days 7, 14, or 21. An IPGTT was performed at days 7 and 14. Mice that were hyperglycemic at day 21 (>11.1 mM) were killed, and the s.c. implants were removed for analysis. Mice that returned to normoglycemia by day 21 were anesthetized, the s.c. modular implant was removed, and the animals were allowed to recover. Blood glucose levels were monitored for the following 2–3 d before the animal was killed; this enabled confirmation that the implant was responsible for the return to normoglycemia. Explants were either sent for histological processing or analyzed using flow cytometry (Fig. S1).

CLARITY Processing and Imaging. GSL-1 (Vector Laboratories) conjugated to Alexa-555 (Thermo Fisher Scientific) was injected via the tail vein of the SCID/bg mouse, and the whole body was perfused as previously described (39). The clarified tissue was imaged using light-sheet microscopy (Zeiss Z1 light-sheet microscope at the Sick Kids Imaging Facility) to generate a 1-mm^3 image, which was then digitally processed using Bitplane IMARIS (version 8.1).

Tissue Digestion and Flow Cytometry. For flow cytometry studies, explants were digested and stained with a panel of markers for inflammatory cells, following previous reports (52). Results were acquired using a five-laser LSR Fortessa X-20 flow cytometer (BD), and data were further analyzed using FlowJo software (v10.0.8).

Detailed materials and methods for our protocols are available in *Supporting Information*.

ACKNOWLEDGMENTS. We thank Chuen Lo for his help and expertise with animal surgeries and islet isolations and Abdullah Muhammad Syed and Shrey Sindhwani of Warren Chan's laboratory at the University of Toronto for helping with imaging our CLARITY-processed tissues. This work was supported by Canadian Institutes of Health Research (CIHR) Grant 142406. A.E.V. and N.C. were supported by scholarships from CIHR and the Province of Ontario. A.E.V. also received funding from the CIHR Training Program for Regenerative Medicine.

1. Shapiro AMJ, et al. (2000) Islet transplantation in seven patients with type 1 diabetes mellitus using a glucocorticoid-free immunosuppressive regimen. *N Engl J Med* 343: 230–238.
2. Berney T, et al. (2009) Long-term insulin-independence after allogeneic islet transplantation for type 1 diabetes: Over the 10-year mark. *Am J Transplant* 9:419–423.
3. Markmann JF, et al. (2003) Insulin independence following isolated islet transplantation and single islet infusions. *Ann Surg* 237:741–749, discussion 749–750.
4. McCall M, Shapiro AM (2012) Update on islet transplantation. *Cold Spring Harb Perspect Med* 2:a007823.
5. Biarnés M, et al. (2002) Beta-cell death and mass in syngeneically transplanted islets exposed to short- and long-term hyperglycemia. *Diabetes* 51:66–72.
6. Shapiro AMJ (2011) Strategies toward single-donor islets of Langerhans transplantation. *Curr Opin Organ Transplant* 16:627–631.
7. Barshes NR, Wyllie S, Goss JA (2005) Inflammation-mediated dysfunction and apoptosis in pancreatic islet transplantation: Implications for intrahepatic grafts. *J Leukoc Biol* 77:587–597.
8. Vériter S, Gianello P, Dufrane D (2013) Bioengineered sites for islet cell transplantation. *Curr Diab Rep* 13:745–755.
9. Coronel MM, Stabler CL (2013) Engineering a local microenvironment for pancreatic islet replacement. *Curr Opin Biotechnol* 24:900–908.
10. Phelps EA, Headen DM, Taylor WR, Thulé PM, García AJ (2013) Vasculogenic bio-synthetic hydrogel for enhancement of pancreatic islet engraftment and function in type 1 diabetes. *Biomaterials* 34:4602–4611.
11. Bhang SH, et al. (2013) Mutual effect of subcutaneously transplanted human adipose-derived stem cells and pancreatic islets within fibrin gel. *Biomaterials* 34:7247–7256.
12. Ludwig B, et al. (2012) Improvement of islet function in a bioartificial pancreas by enhanced oxygen supply and growth hormone releasing hormone agonist. *Proc Natl Acad Sci USA* 109:5022–5027.
13. Pepper AR, et al. (2015) A prevascularized subcutaneous device-less site for islet and cellular transplantation. *Nat Biotechnol* 33:518–523.
14. Pepper AR, et al. (2015) Diabetes is reversed in a murine model by marginal mass syngeneic islet transplantation using a subcutaneous cell pouch device. *Transplantation* 99:2294–2300.
15. Pepper AR, Gala-Lopez B, Ziff O, Shapiro AMJ (2013) Revascularization of transplanted pancreatic islets and role of the transplantation site. *Clin Dev Immunol* 2013: 352315.
16. Zhang N, et al. (2004) Elevated vascular endothelial growth factor production in islets improves islet graft vascularization. *Diabetes* 53:963–970.
17. Nyqvist D, et al. (2011) Donor islet endothelial cells in pancreatic islet revascularization. *Diabetes* 60:2571–2577.
18. McGuigan AP, Sefton MV (2006) Vascularized organoid engineered by modular assembly enables blood perfusion. *Proc Natl Acad Sci USA* 103:11461–11466.
19. Chamberlain MD, Gupta R, Sefton MV (2012) Bone marrow-derived mesenchymal stromal cells enhance chimeric vessel development driven by endothelial cell-coated microtissues. *Tissue Eng Part A* 18:285–294.
20. Butler MJ, Sefton MV (2012) Cotransplantation of adipose-derived mesenchymal stromal cells and endothelial cells in a modular construct drives vascularization in SCID/bg mice. *Tissue Eng Part A* 18:1628–1641.
21. Tomer R, Ye L, Hsueh B, Deisseroth K (2014) Advanced CLARITY for rapid and high-resolution imaging of intact tissues. *Nat Protoc* 9:1682–1697.
22. Yang B, et al. (2014) Single-cell phenotyping within transparent intact tissue through whole-body clearing. *Cell* 158:945–958.
23. Hammar E, et al. (2004) Extracellular matrix protects pancreatic beta-cells against apoptosis: Role of short- and long-term signaling pathways. *Diabetes* 53:2034–2041.
24. Zhao Y, et al. (2010) Preservation of islet survival by upregulating α3 integrin signaling: The importance of 3-dimensional islet culture in basement membrane extract. *Transplant Proc* 42:4638–4642.
25. Yap WT, et al. (2013) Collagen IV-modified scaffolds improve islet survival and function and reduce time to euglycemia. *Tissue Eng Part A* 19:2361–2372.
26. Fumimoto Y, et al. (2009) Creation of a rich subcutaneous vascular network with implanted adipose tissue-derived stromal cells and adipose tissue enhances subcutaneous grafting of islets in diabetic mice. *Tissue Eng Part C Methods* 15:437–444.
27. Sakata N, Chan NK, Chrisler J, Obenaus A, Hathout E (2010) Bone marrow cell co-transplantation with islets improves their vascularization and function. *Transplantation* 89: 686–693.
28. Buitinga M, et al. (2016) Coculturing human islets with proangiogenic support cells to improve islet revascularization at the subcutaneous transplantation site. *Tissue Eng Part A* 22:375–385.
29. Christoffersson G, et al. (2012) VEGF-A recruits a proangiogenic MMP-9-delivering neutrophil subset that induces angiogenesis in transplanted hypoxic tissue. *Blood* 120:4653–4662.
30. Hirabaru M, et al. (2015) A method for performing islet transplantation using tissue-engineered sheets of islets and mesenchymal stem cells. *Tissue Eng Part C Methods* 21:1205–1215.
31. Ellis C, Suuronen E, Yeung T, Seeberger K, Korbutt G (2014) Bioengineering a highly vascularized matrix for the ectopic transplantation of islets. *Islets* 5:216–225.
32. Perez-Basterrechea M, et al. (2009) Plasma-fibroblast gel as scaffold for islet transplantation. *Tissue Eng Part A* 15:569–577.
33. Iuamoto LR, et al. (2017) Human islet xenotransplantation in rodents: A literature review of experimental model trends. *Clinics (Sao Paulo)* 72:238–243.
34. Luan NM, Iwata H (2014) Long-term allogeneic islet graft survival in prevascularized subcutaneous sites without immunosuppressive treatment. *Am J Transplant* 14: 1533–1542.
35. Pepper AR, et al. (2016) Harnessing the foreign body reaction in marginal mass device-less subcutaneous islet transplantation in mice. *Transplantation* 100: 1474–1479.
36. Brehm MA, et al. (2010) Human immune system development and rejection of human islet allografts in spontaneously diabetic NOD-Rag1null IL2rgammanull Ins2Akita mice. *Diabetes* 59:2265–2270.
37. Biessels GJ, et al. (2014) Phenotyping animal models of diabetic neuropathy: A consensus statement of the diabetic neuropathy study group of the EASD (Neurodiab). *J Peripher Nerv Syst* 19:77–87.
38. Cabrera O, et al. (2006) The unique cytoarchitecture of human pancreatic islets has implications for islet cell function. *Proc Natl Acad Sci USA* 103:2334–2339.
39. Sindhwani S, et al. (2016) Three-dimensional optical mapping of nanoparticle distribution in intact tissues. *ACS Nano* 10:5468–5478.
40. Chen YY, et al. (2016) Clarifying intact 3D tissues on a microfluidic chip for high-throughput structural analysis. *Proc Natl Acad Sci USA* 113:14915–14920.
41. West M, Sefton MV (2016) Enhanced vascularization of modular engineered tissues using activated macrophages. PhD thesis (University of Toronto, Toronto). pp 1–70.
42. Johansson U, Elgue G, Nilsson B, Korsgren O (2005) Composite islet-endothelial cell grafts: A novel approach to counteract innate immunity in islet transplantation. *Am J Transplant* 5:2632–2639.
43. Negi S, et al. (2012) Analysis of beta-cell gene expression reveals inflammatory signaling and evidence of dedifferentiation following human islet isolation and culture. *PLoS One* 7:e30415.
44. Brissova M, et al. (2014) Islet microenvironment, modulated by vascular endothelial growth factor-A signaling, promotes β cell regeneration. *Cell Metab* 19:498–511.
45. Ortega-Gómez A, Perretti M, Soehnlein O (2013) Resolution of inflammation: An integrated view. *EMBO Mol Med* 5:661–674.
46. Parsa R, et al. (2012) Adoptive transfer of immunomodulatory M2 macrophages prevents type 1 diabetes in NOD mice. *Diabetes* 61:2881–2892.
47. Xiao X, et al. (2014) M2 macrophages promote beta-cell proliferation by up-regulation of SMAD7. *Proc Natl Acad Sci USA* 111:E1211–E1220.
48. Doloff JC, et al. (2017) Colony stimulating factor-1 receptor is a central component of the foreign body response to biomaterial implants in rodents and non-human primates. *Nat Mater* 16:671–680.
49. Wu DC, et al. (2013) Ex vivo expanded human regulatory T cells can prolong survival of a human islet allograft in a humanized mouse model. *Transplantation* 96:707–716.
50. Carter JD, Dula SB, Corbin KL, Wu R, Nunemaker CS (2009) A practical guide to rodent islet isolation and assessment. *Biol Proced Online* 11:3–31.
51. Quaranta P, et al. (2014) Co-transplantation of endothelial progenitor cells and pancreatic islets to induce long-lasting normoglycemia in streptozotocin-treated diabetic rats. *PLoS One* 9:e94783.
52. Lisovsky A, Zhang DKY, Sefton MV (2016) Effect of methacrylic acid beads on the sonic hedgehog signaling pathway and macrophage polarization in a subcutaneous injection mouse model. *Biomaterials* 98:203–214.
53. Staudt T, Lang MC, Medda R, Engelhardt J, Hell SW (2007) 2,2′-thiodiethanol: A new water soluble mounting medium for high resolution optical microscopy. *Microsc Res Tech* 70:1–9.
54. Games PA, Howell JF (1976) Pairwise multiple comparison procedures with unequal N's and/or variances: A Monte Carlo study. *J Educ Stat* 1:113–125.